The X-ray hard lag in Cyg X-1 – can they be explained by Compton scattering?

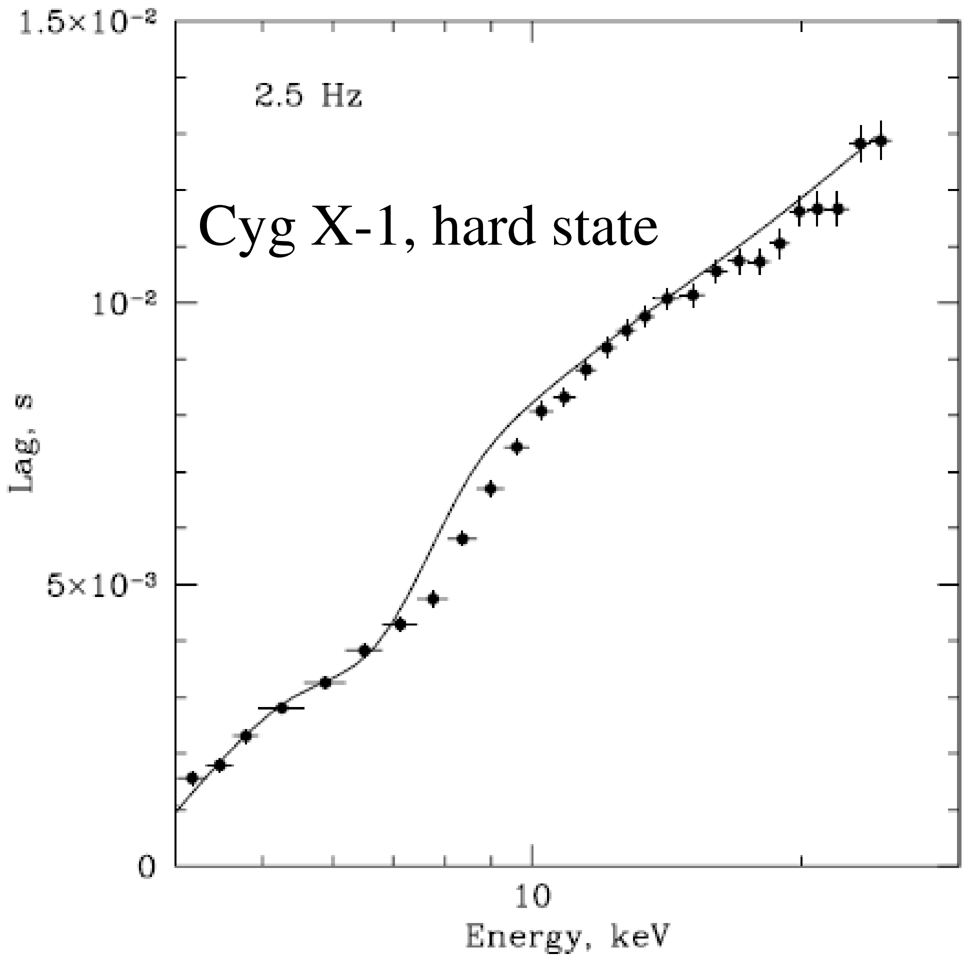

Kotov+ 2001

The observed lags are usually explained by fluctuations propagating with the accretion flow (Lyubarsky 1997; Arevalo & Uttley 2006, Ingram & Done 2012), and the local spectrum hardening with the decreasing radius.

Kazanas, Hua & Titarchuk (1997) proposed they are explained by Compton scattering in a very large corona, $>10^{10}$ cm.

The width of the auto-correlation decreases with increasing energy band

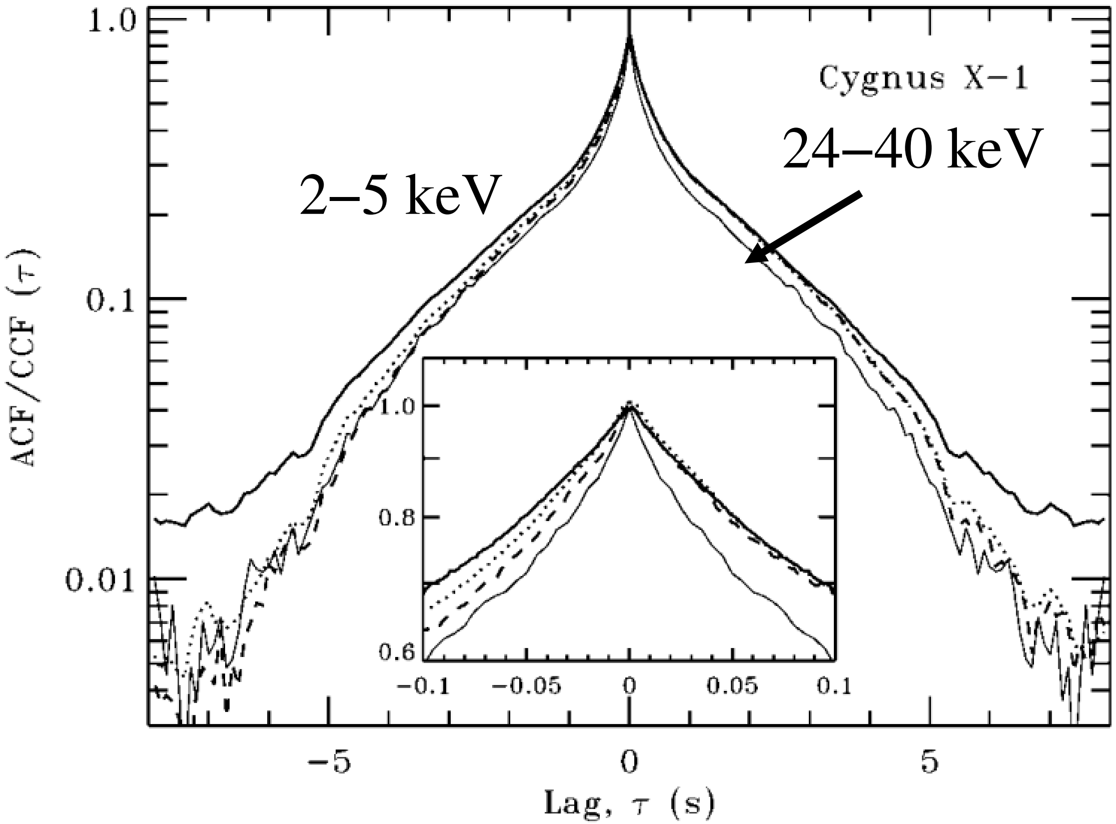

Maccarone+2000

Also, as noted by Nowak+1999, the observed dependence on the Fourier frequency is not compatible with a single corona. The Compton model is ruled out.

Non-uniqueness of reflection spectral fitting. Two examples for BH binaries.

A controversy regarding the truncation radii in the hard state: the case of GX 339–4

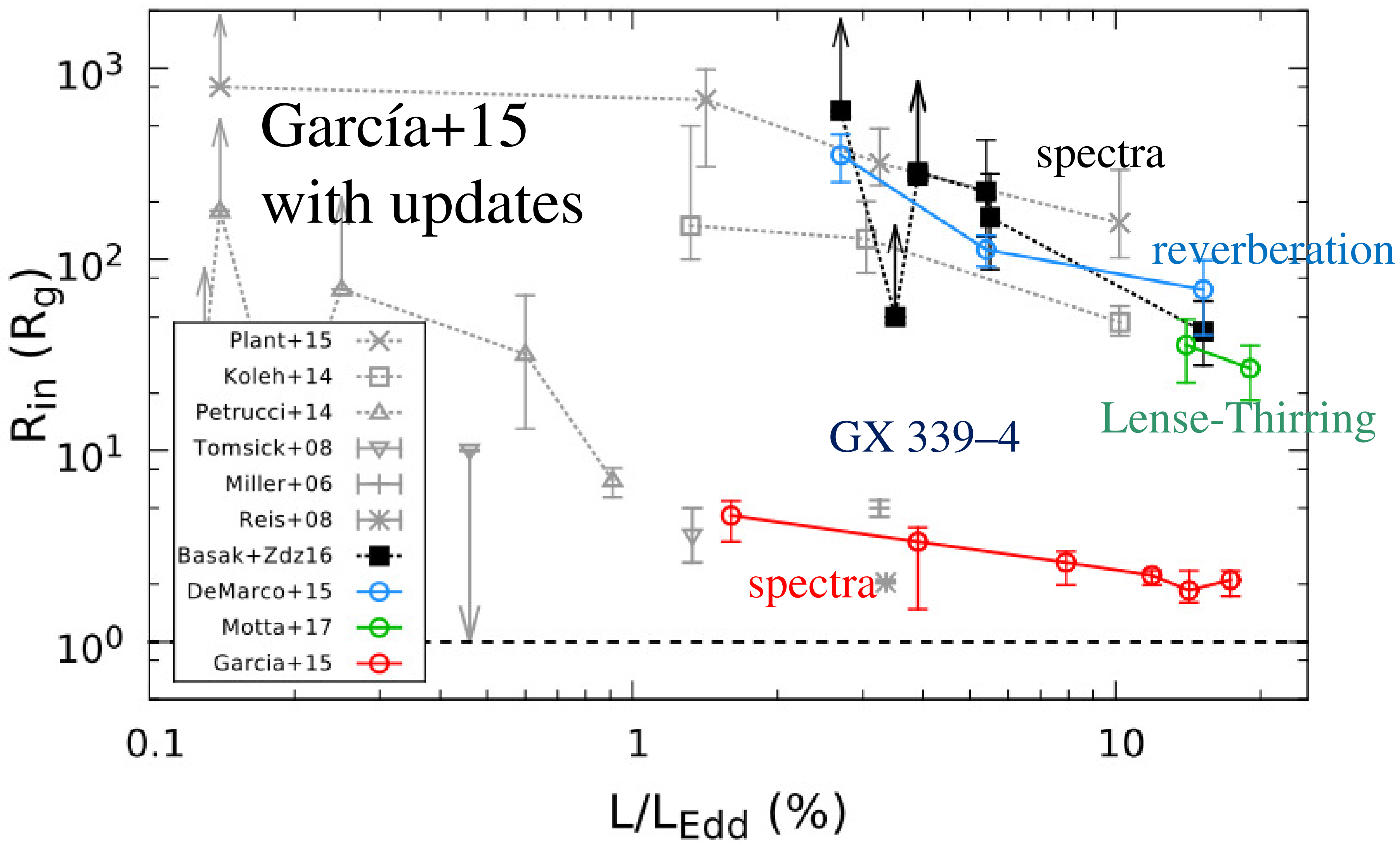

The absence of truncation?

The main arguments for the presence of a cold accretion disc extending close to ISCO and a very compact corona in the hard state are observations of broad Fe K lines (e.g. Miller+2006; Reis+2008, 2009; Rykoff+2007; Garcia+2015; Parker+2015; Wang-ji+2018 and many other papers).

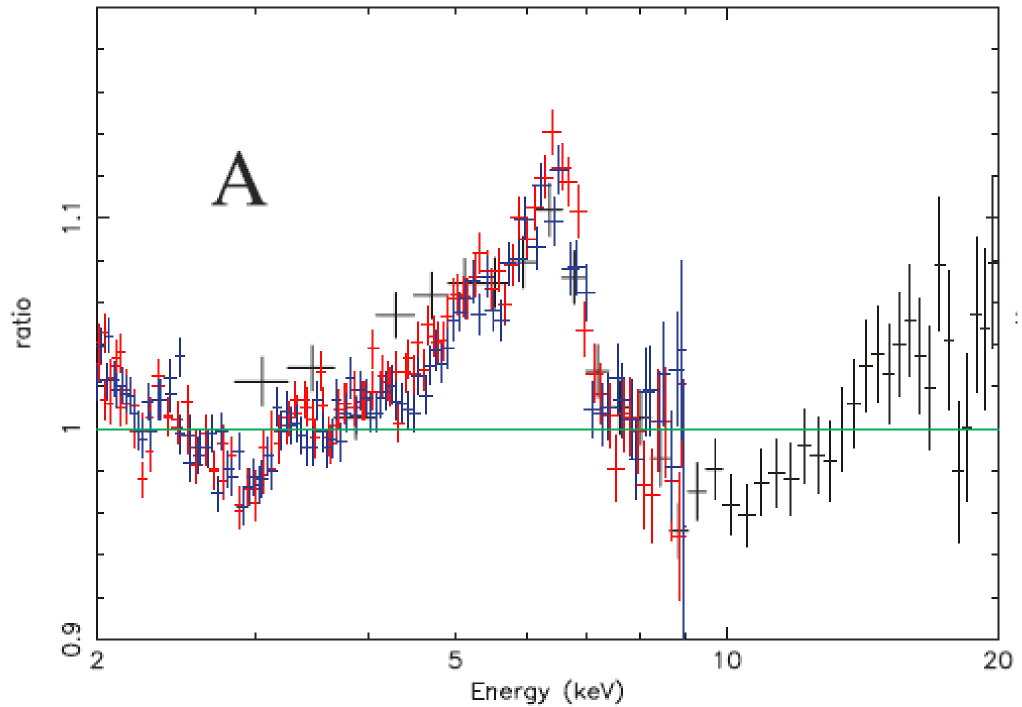

GX 339–4

What causes the conflicting measurements?

- Calibration uncertainties.
- Pileup in the detector.
- Uncertainty about the underlying continuum. A hard continuum below the Fe K line requires a strong red wing of the line, thus, implying strong relativistic effects. A soft continuum may be compatible with a narrow line. In general, the X-ray continuum is unlikely to be a single power law.
- Other causes of the broadening? Compton scattering in the upper disc layers? The assumption of constant density vs. hydrostatic equilibrium?

E.g., results by Done & Diaz Trigo (2010)

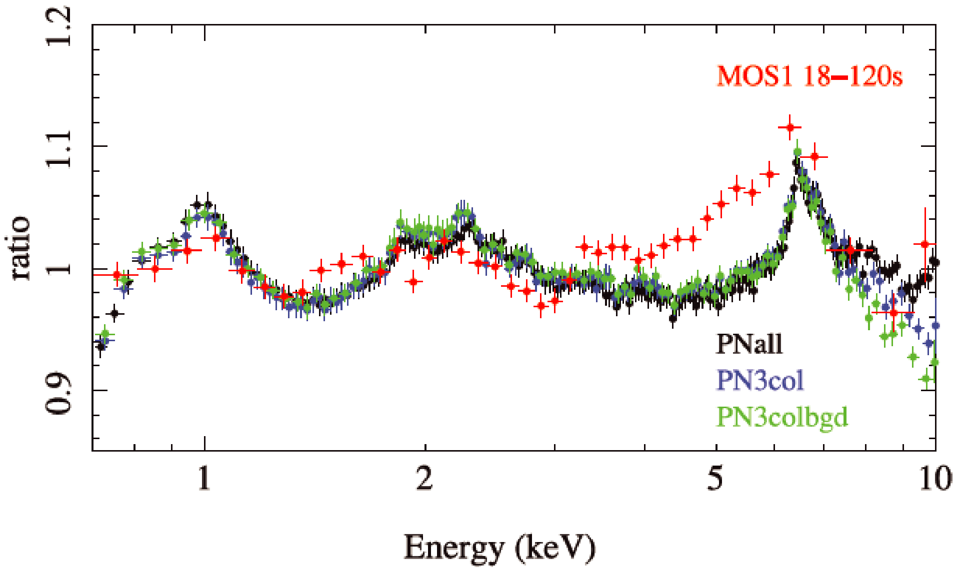

- Strong pileup in the *XMM* MOS detector. The Fe Kα line much narrower when measured with the *XMM* EPIC-pn detector.

The inner disc radius and reflection in GX 339–4 from *XMM* data (Basak & AAZ 2016)

The values of the inner disc radius between tens and hundreds of the gravitational radius, R_g, and the reflection fractions ≤1. The inner radius increases with the increasing hardness, and the reflection fraction decreases.

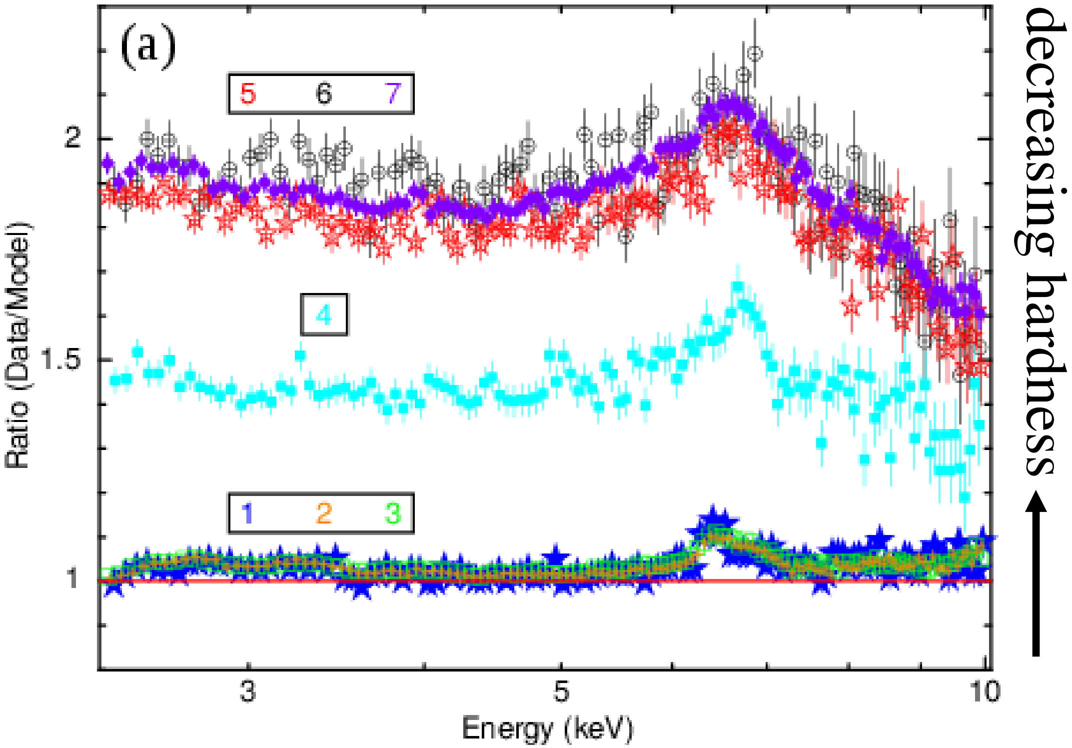

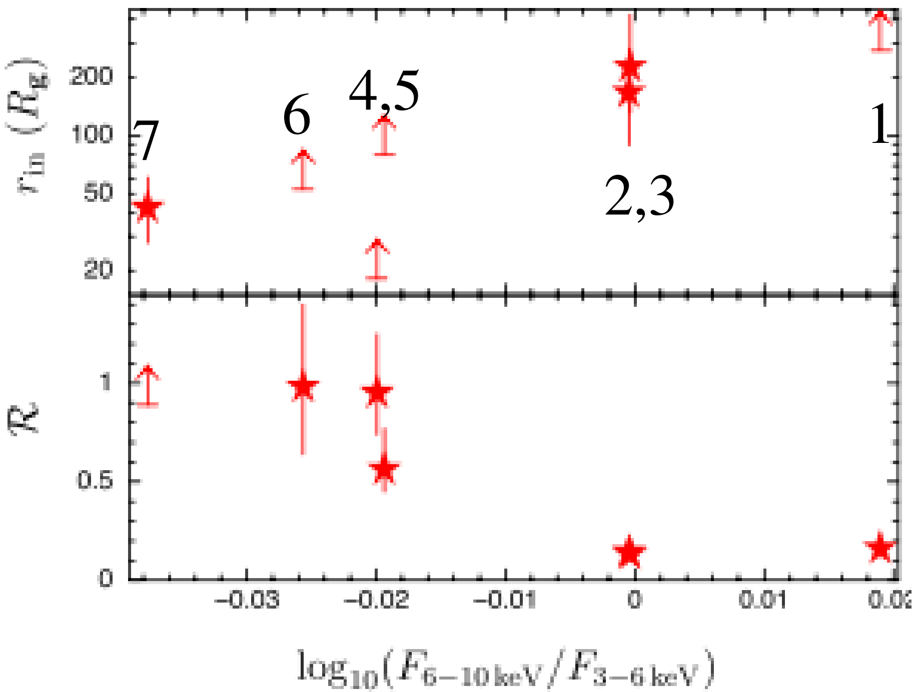

tbnew_feo(diskbb + nthcomp + relxill)

Strong broadening seen in the model spectra for high ionization parameters

- A non-relativistic effect.
- It is due to a reduced absorption cross section at a sufficiently high ionization level.
- Incoming photons can penetrate deep in the medium before they ionize a K shell of a Fe atom, and a Fe Kα line is formed.
- The line then undergoes repeated scattering in warm/hot disc upper layers before it leaves the disc, and becomes broad.

Reflection spectra from static ionized medium

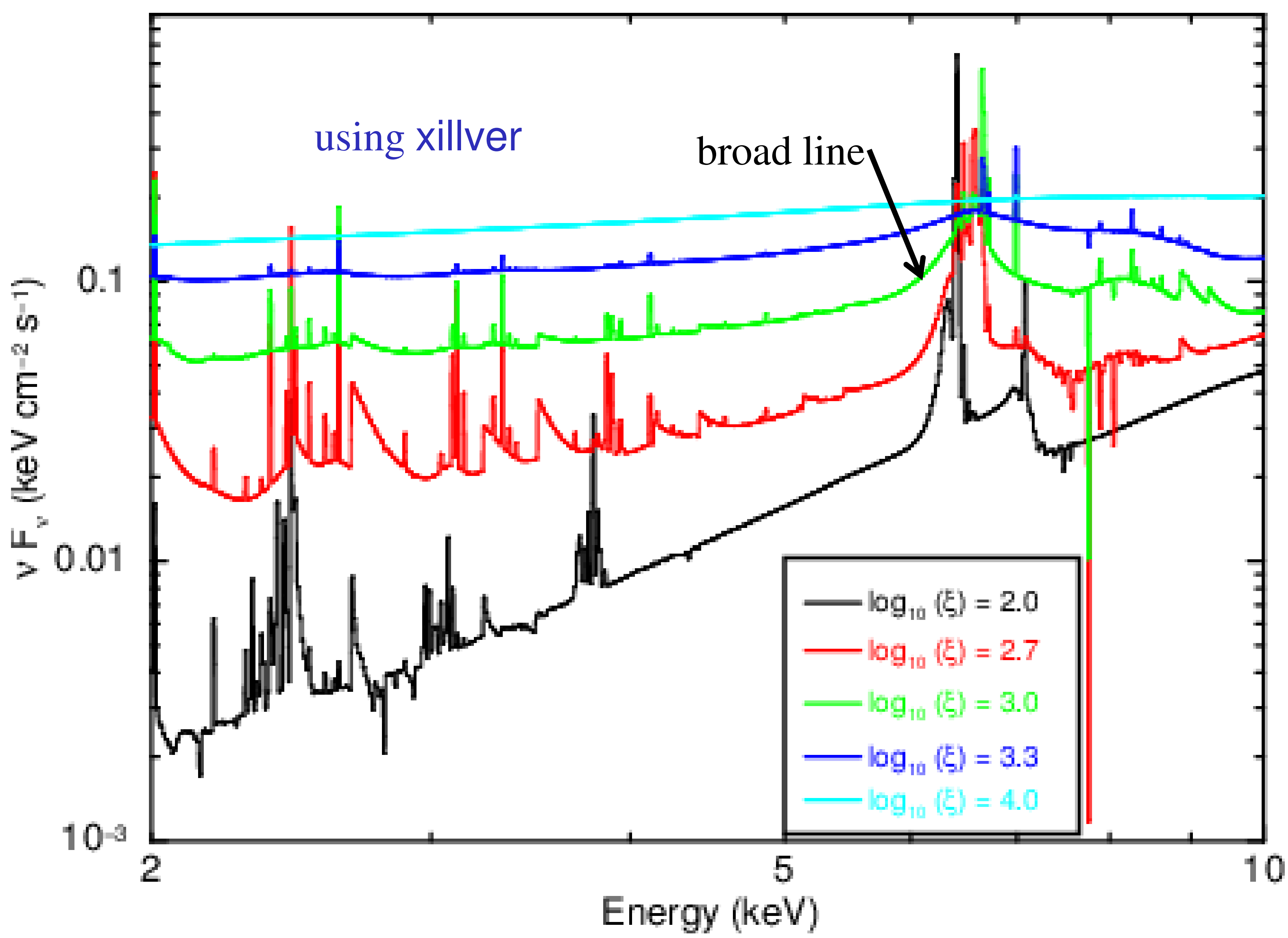

The same, including a modest relativistic broadening

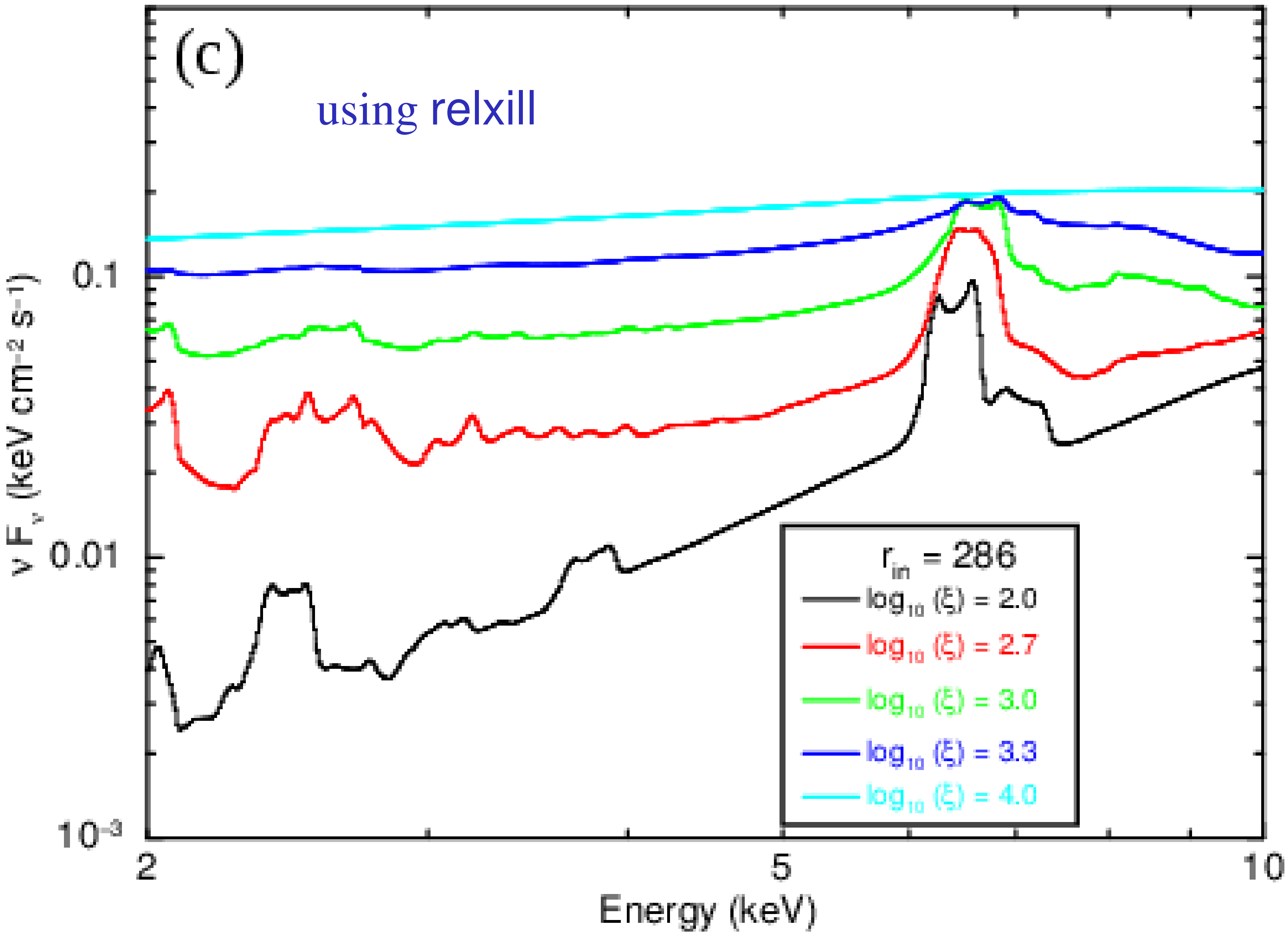

The nature of the soft component

- Our model was tbnew_feo(diskbb + nthcomp + relxill).
- But diskbb here does not describe a standard accretion disc.
- We have tried to tie the inner radius of the diskbb (by modifying it) to the inner radius of relxill, but got the unlikely result of R_{in} increasing with increasing L and decreasing hardness:

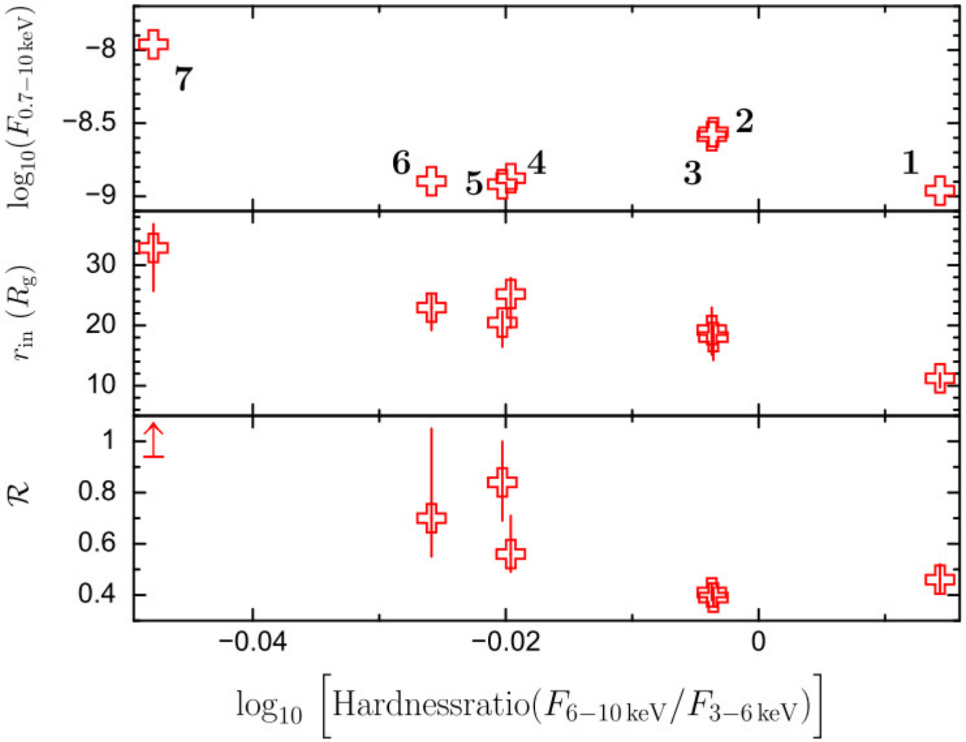

The nature of the soft component

- In the hard state, most of the power is in the hard (presumably Compton) component, not in the disc.
- The hard component irradiates the disc, and emission from the reprocessing is likely to be > that from internal dissipation.

Cyg X-1: typical hard state spectrum fitted by the truncated disc model

$\frac{L_{\rm hot}}{L_{\rm disk}} \gg 1$

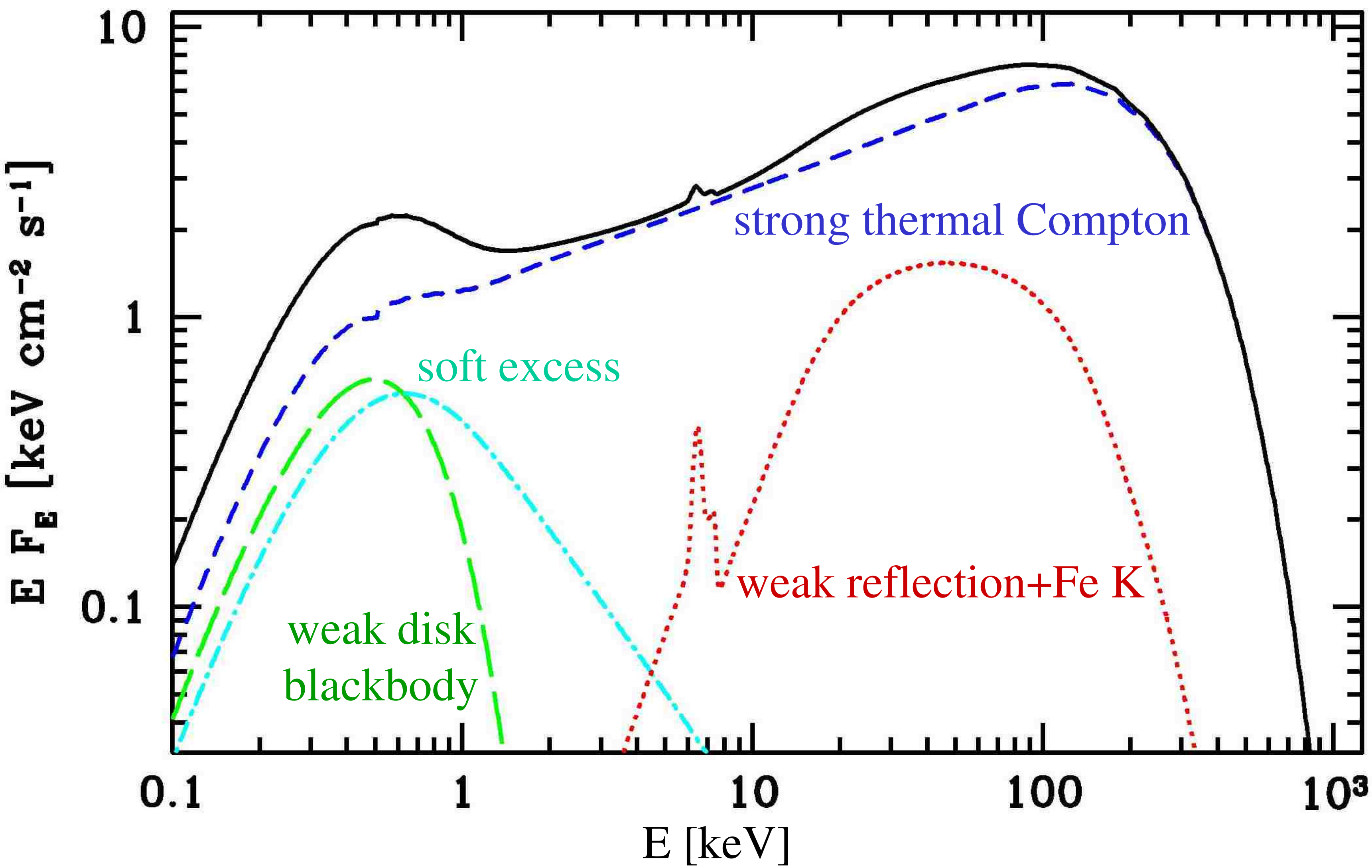

AAZ & Gierliński 2004

$kT \approx 50$–100 keV, $\tau_T \sim 1$, $\Omega/2\pi \approx 0.3$, $L \approx 1$–2% of L_E

Cyg X-1 hard state

- Simultaneous *Suzaku*/*NuSTAR* observation of in 2014.
- Studied by Parker+ 2015, who found as their best fit a lamppost model with the disc $R_{\rm in} \approx R_{\rm ISCO}$ and a very low height of the lamppost:

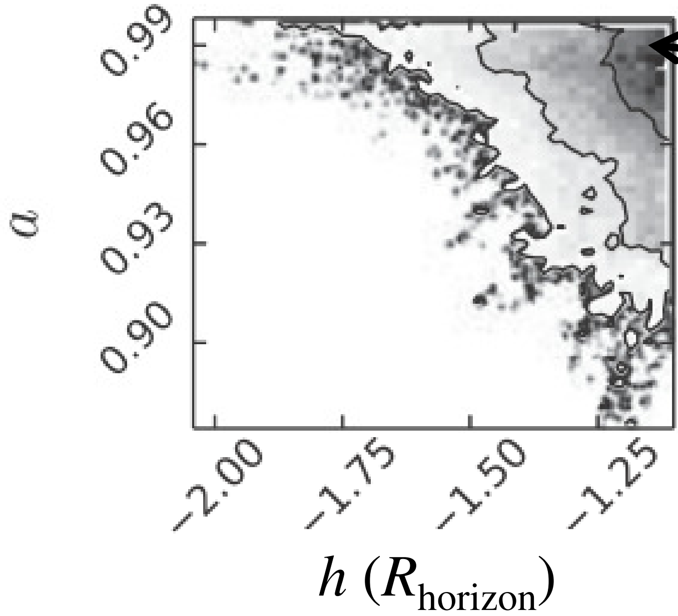

best fit close to $a \approx 1$, $h \approx 1$.

The incident continua in Cyg X-1 assumed by Parker+2015 and Basak+2017

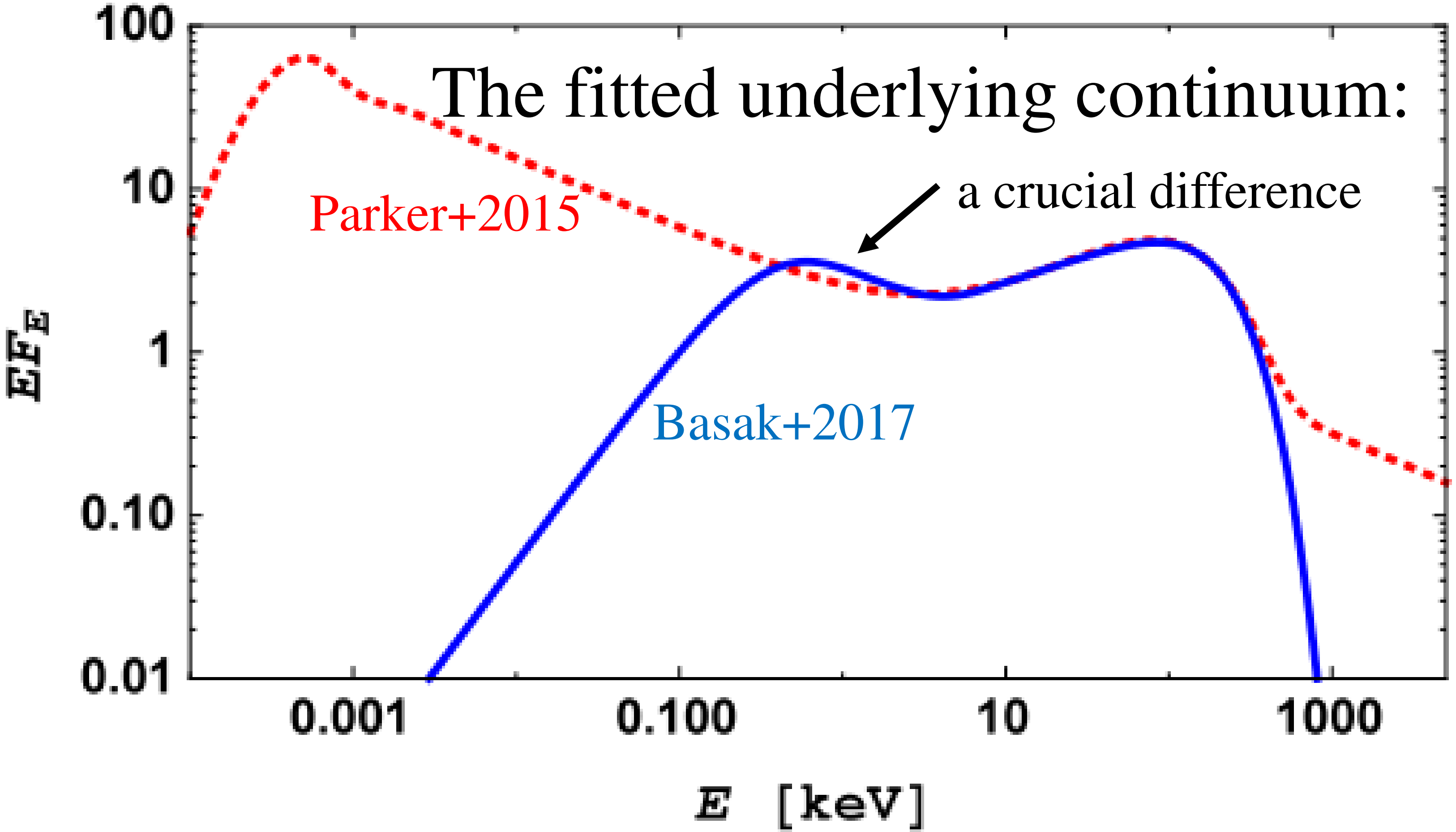

Parker+ used the eqpair model for a very low compactness parameter, *L*/*R*, implying the source size of ~3×10^{11} cm, and assuming the disc $kT\approx0.2$ eV. The hard component in their model is due to thermal bremsstrahlung.

A reanalysis of *NuSTAR-Suzaku* data for Cyg X-1 in the hard state

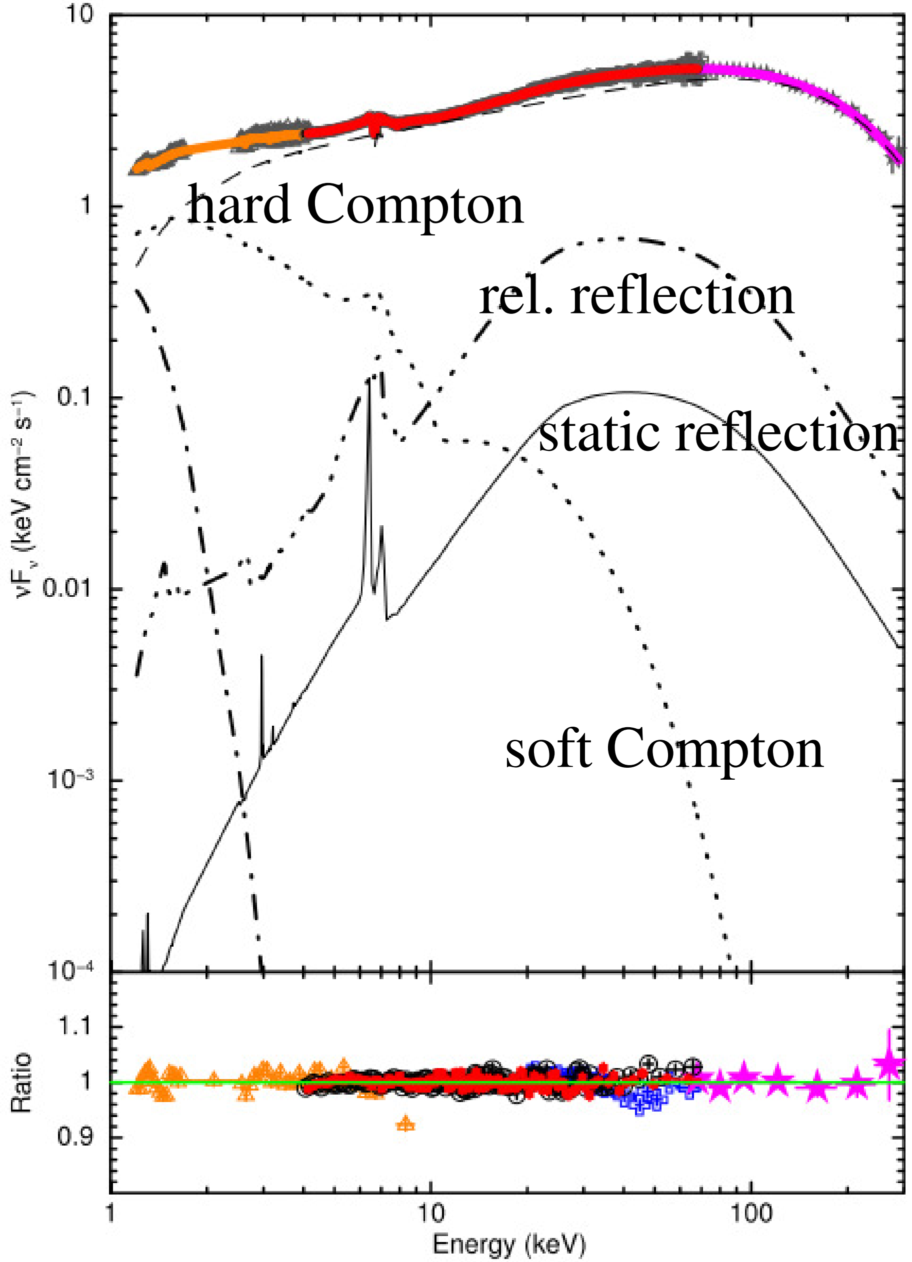

Basak, AAZ, Parker & Islam (2017)

The same data set as in Parker+2015, who found $r_{\rm in} \approx 1.5\pm0.3\ r_{\rm ISCO}$ (a>0.97). We include a 2nd soft Comptonization component (e.g., Yamada+2013) and also find weak reflection, but $r_{\rm in} \approx 15\pm3\ r_{\rm g}$ (truncated disc). The present fit is better, χ_ν^2=1216/1001, than the previous one, χ_ν^2=1232/1000.

The data show a soft excess regardless of the fitted model.

The effect of soft excess on reflection fits

- Reflection fits strongly depend on the underlying continuum, which is concave in the presence of a soft excess, which in turn decreases the red wing of the line.
- In Cyg X-1, soft excess was found in e.g. Di Salvo+01, Frontera+01, Makishima+08, Nowak+11, Yamada+13, Basak+17.
- Such excess can significantly reduce the strength and width of the Fe K line, e.g., from EW=1.4 keV (Reynold 1997) to 30 eV in 3C 382 (Woźniak, AAZ+1998).

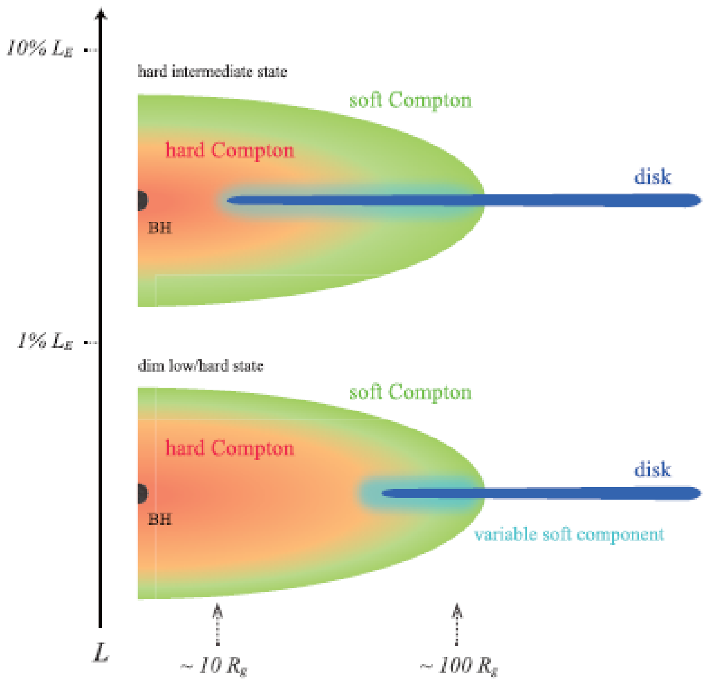

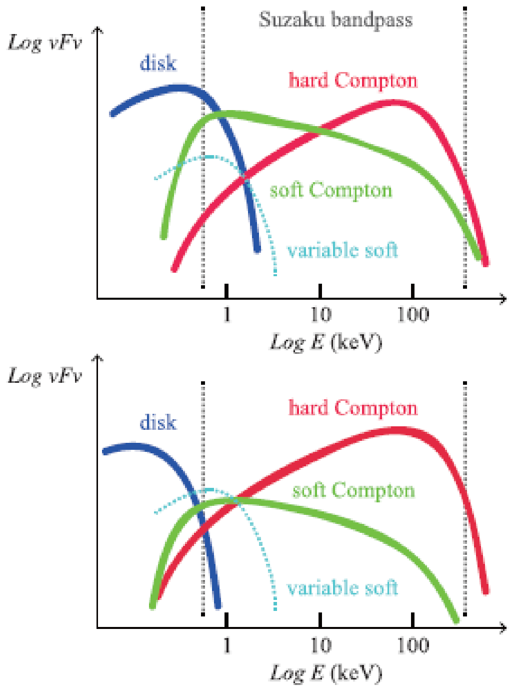

Soft excess in GX 339–4

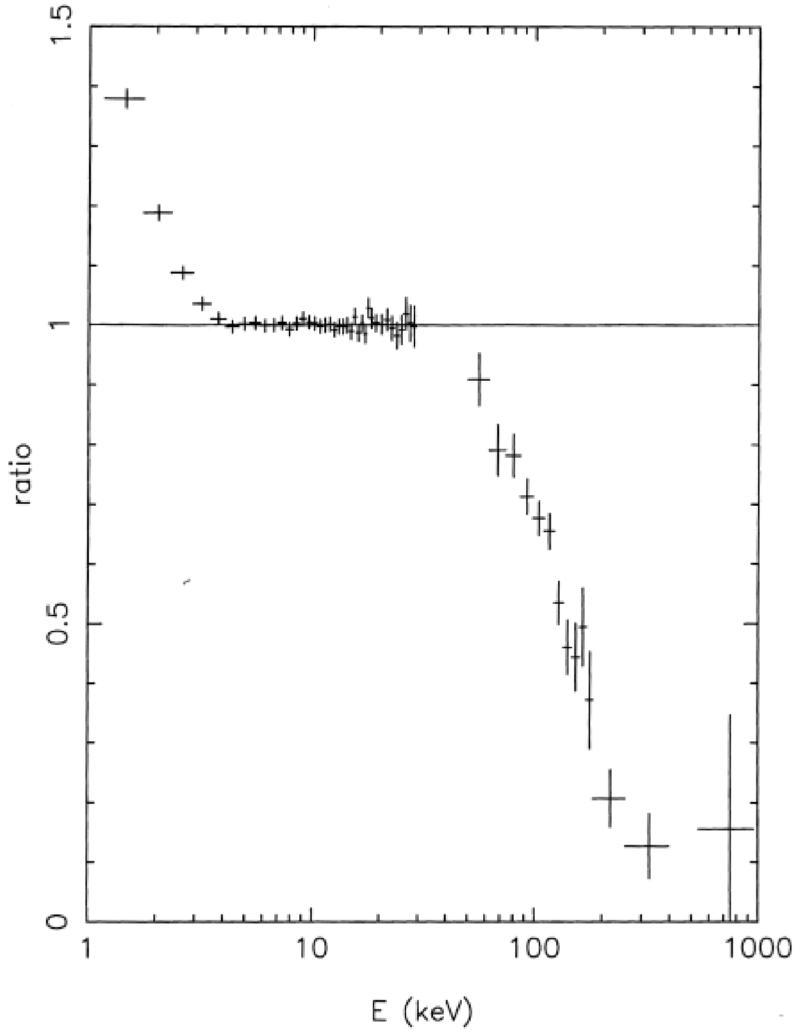

AAZ+98

Figure 3. The ratio of the data of 1991 September 11 from *Ginga* and OSSE to the model consisting of a power law, Compton reflection and an Fe Kα line fitted to the *Ginga* data in the 4.1–29 keV energy range.

An additonal effect: power-law index variability:

Is the average direct emission a straight power law?

The fractional variability, rms, is decreasing with energy in the hard state:

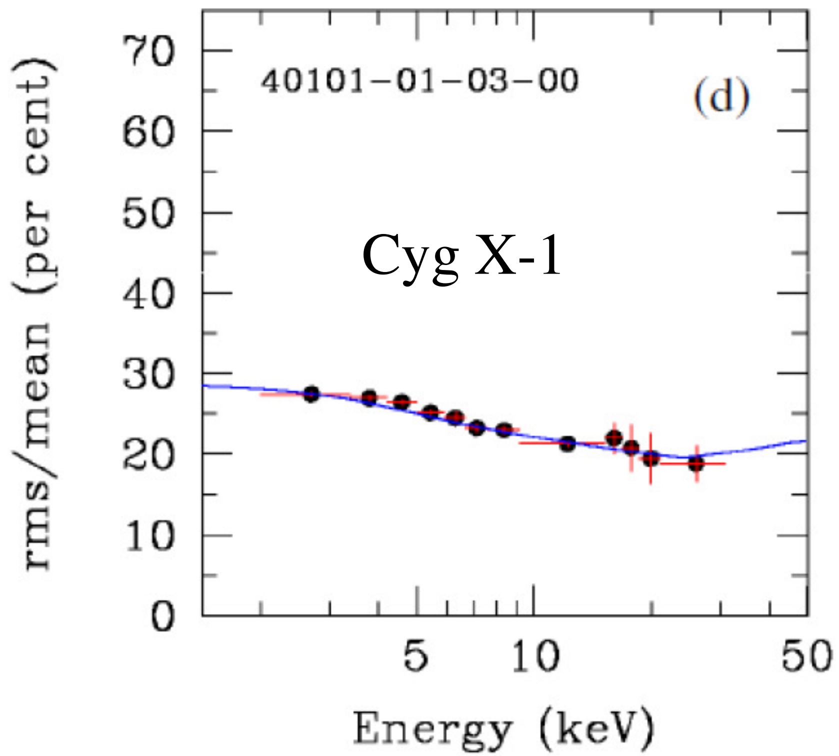

A model: pivoting variability driven by changes in the soft-photon input:

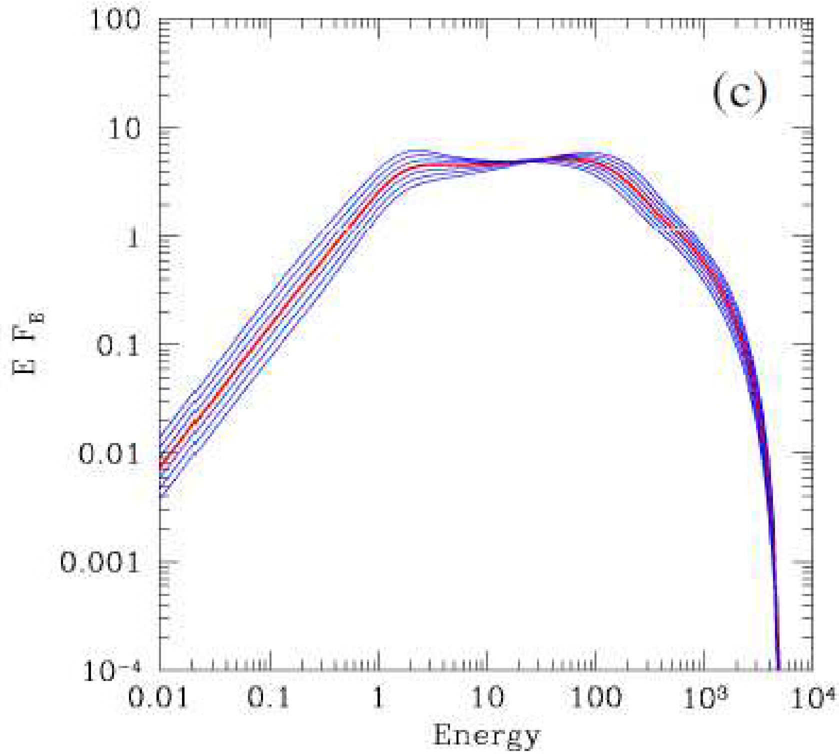

Thus, the average spectrum is not a power law, it is concave, which would reduce the strength of the fitted line.

Gierliński, AAZ & Done 2010

New improved codes for relativistic reflection

- reflkerr – coronal geometry, reflkerr_lp – lampost, + a version of reflection of neutron-star boundary layer emission.
- Improvements with respect to the popular relxill codes (many papers by Dauser et al. and García et al.):
- The incident continuum: thermal Comptonization valid at most temperatures of interest (Poutanen & Svensson 1996).
- Reflection including Klein-Nishina.
- The atomic physics: xillver of García & Kallman 2010.
- Lamppost, both sources treated.
- Full agreement with kynrefrev (Dovčiak +2004), but some differences with respect to relxill.
- See Niedźwiecki, Szanecki & AAZ 2019, Niedźwiecki & AAZ 2018, Niedźwiecki, AAZ & Szanecki 2016 for details.

The effect of the bottom source in the lamppost model (included in reflkerr)

Niedźwiecki & AAZ 2018

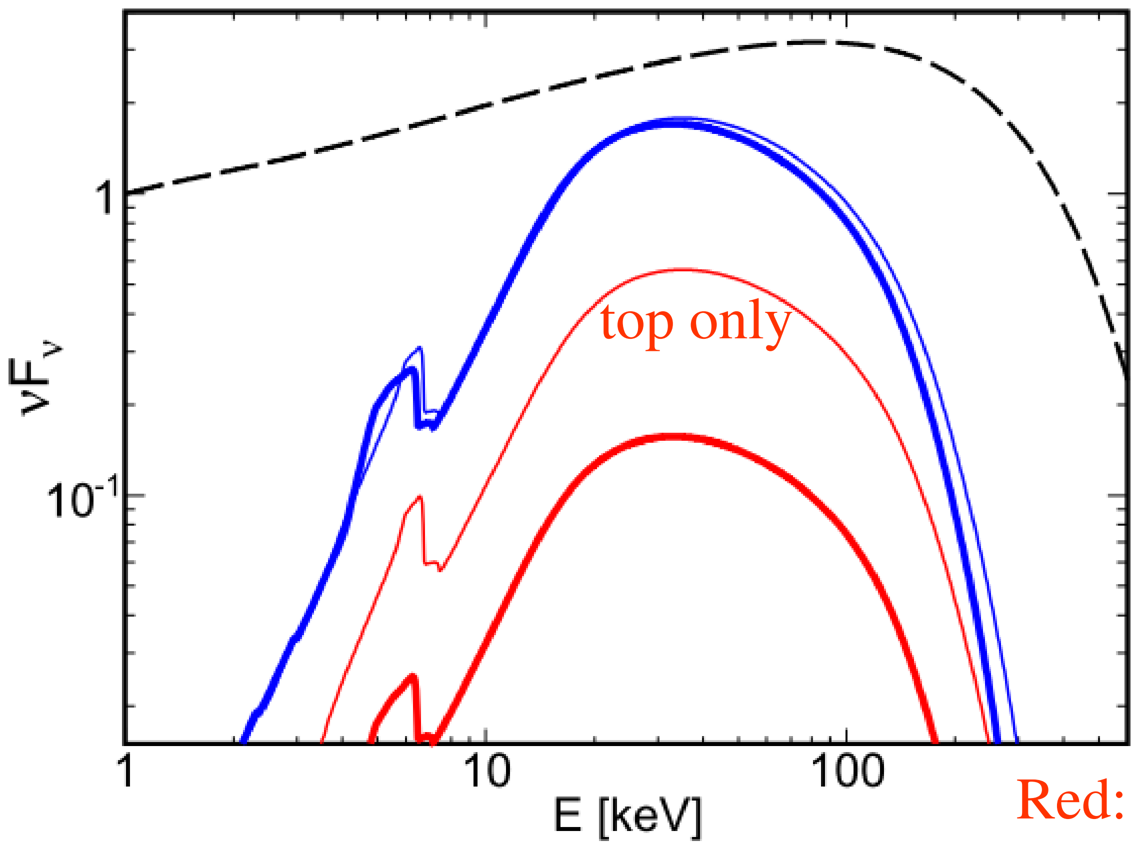

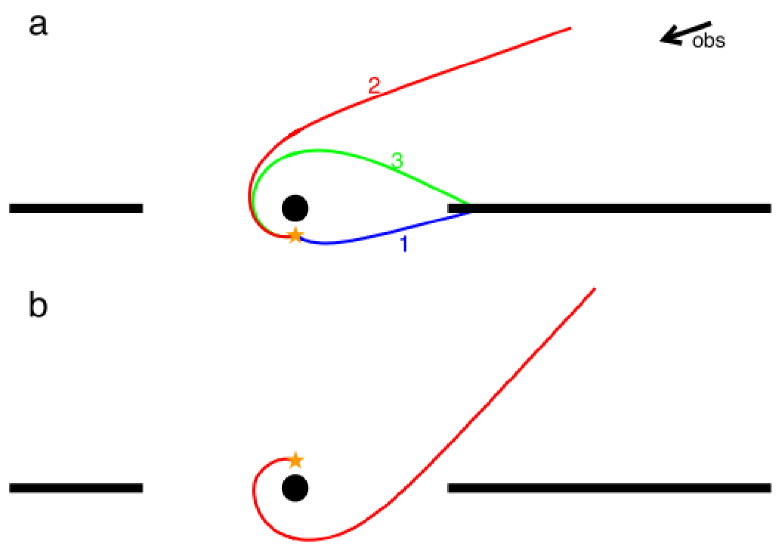

Red: θ=9°, blue: θ=30°. h=2, r_{in}=4.9 [R_g]

The BH is a gravitaional lense, enhancing the direct emission of the bottom source. Here, we normalize the spectra to the incident one. Thus, that enhancement is seen as a reduction in the reflection amplitude.

Flux reduction of the lamppost radiation – extreme for small heights

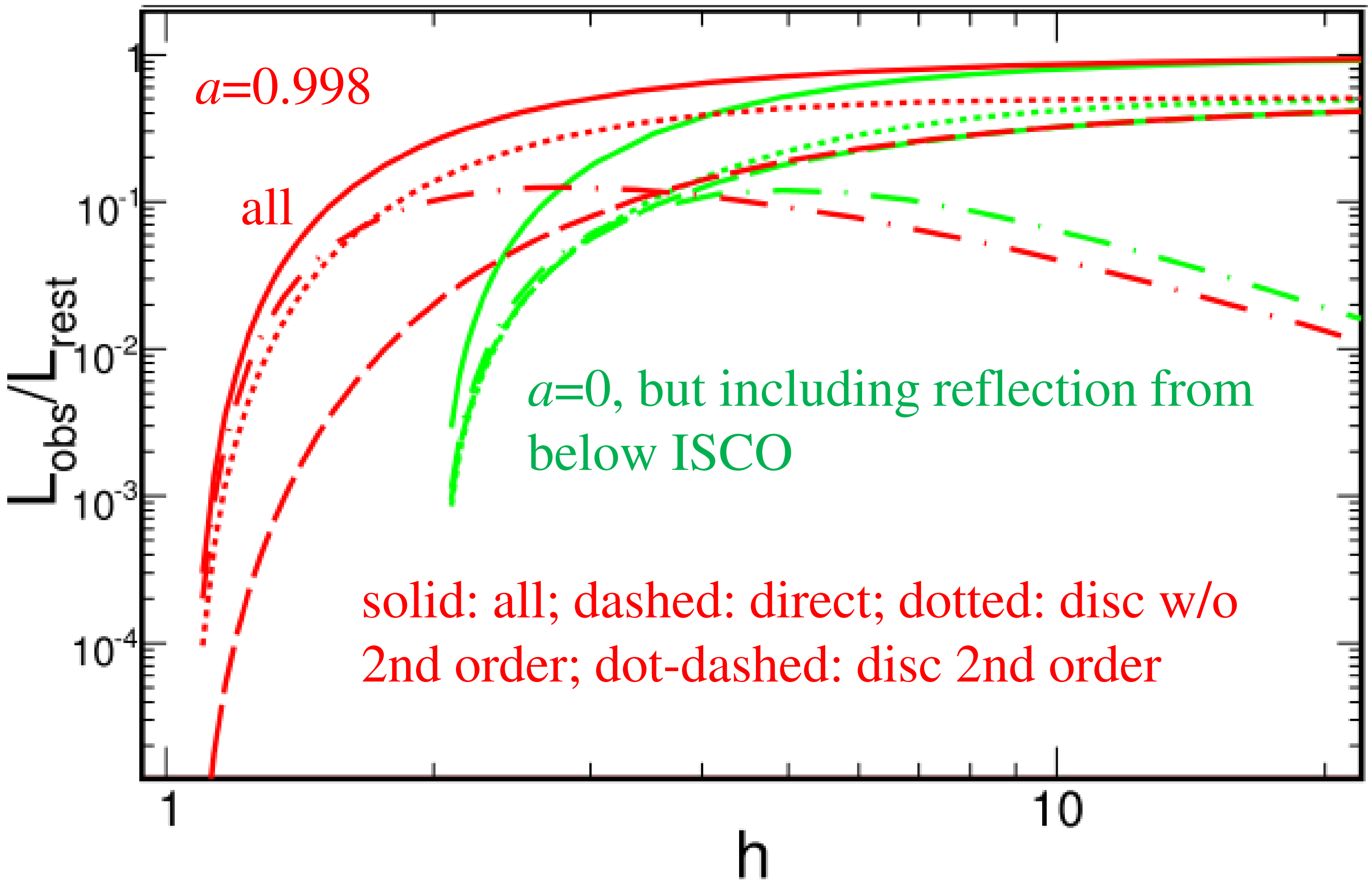

Importance of higher-order reflection, of reflected radiation returning to the disc

Niedźwiecki & AAZ 2018

An example of reflection of emission of the boundary layer of a neutron star

Observed spectra

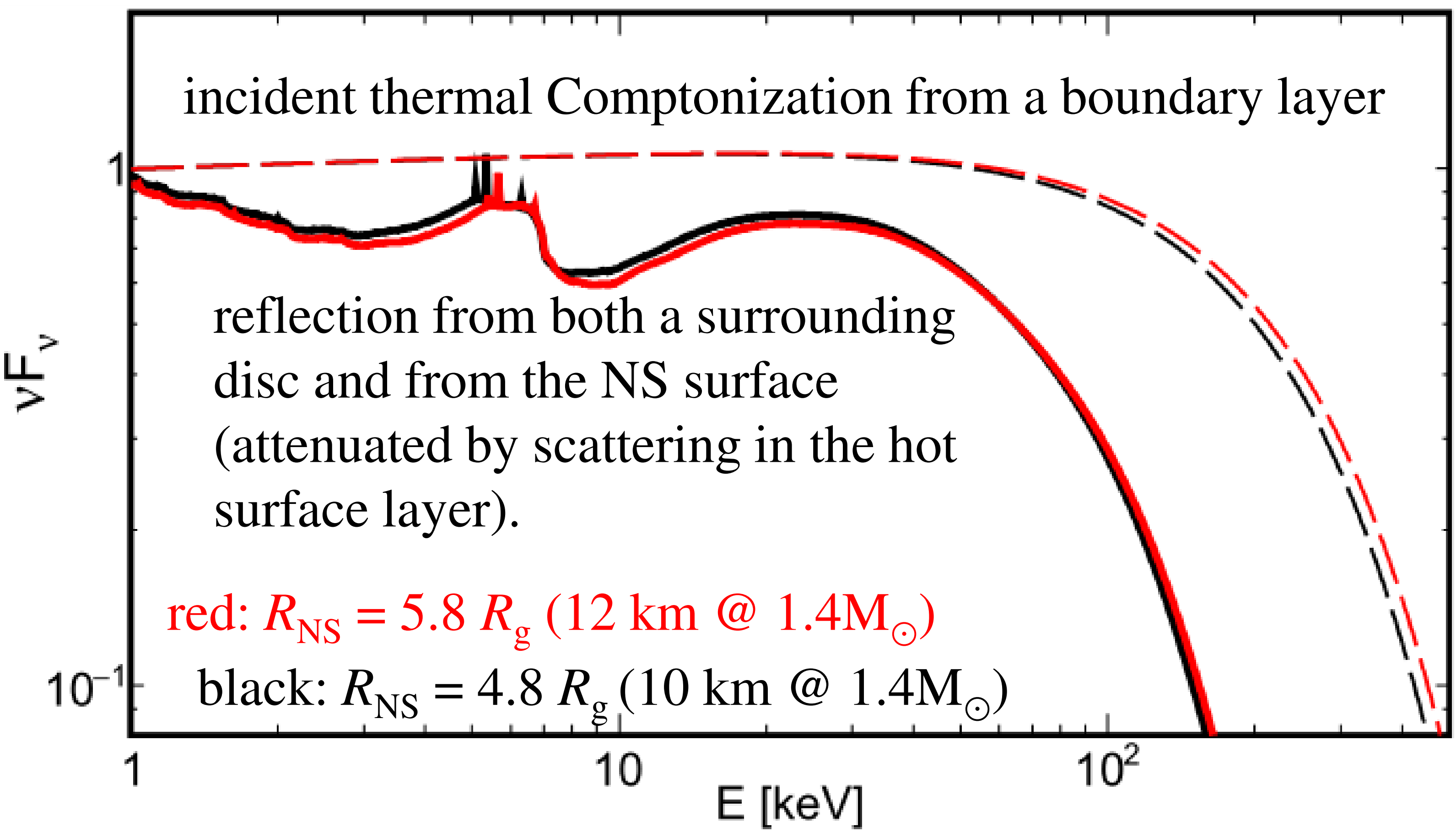

Controversies regarding the hard state

- Disputed geometry and components, either:
  1. X-ray emission from accretion.
  2. X-ray emission from a jet.
- Different possible accretion geometries, either:
  1. a hot inner flow overlapping with a truncated outer disc;
  2. a hot inner flow containing blobs or a residual inner disc;
  3. a standard disc extending to ISCO with a corona;
  4. a standard disc extending to ISCO with a lamppost.

Time lags from blackbody disc reverberation

- A central X-ray source irradiates optically-thick surrounding material (disc), which then reradiates the absorbed photons as blackbody.
- De Marco+2015 found from light-travel time lags the disc truncation radius in GX 339–4 decreasing from ~300 to ~50r_g as the bolometric luminosity increases from 3% to 15% of L_{Edd}.
- Even longer lags found in H1743–322.

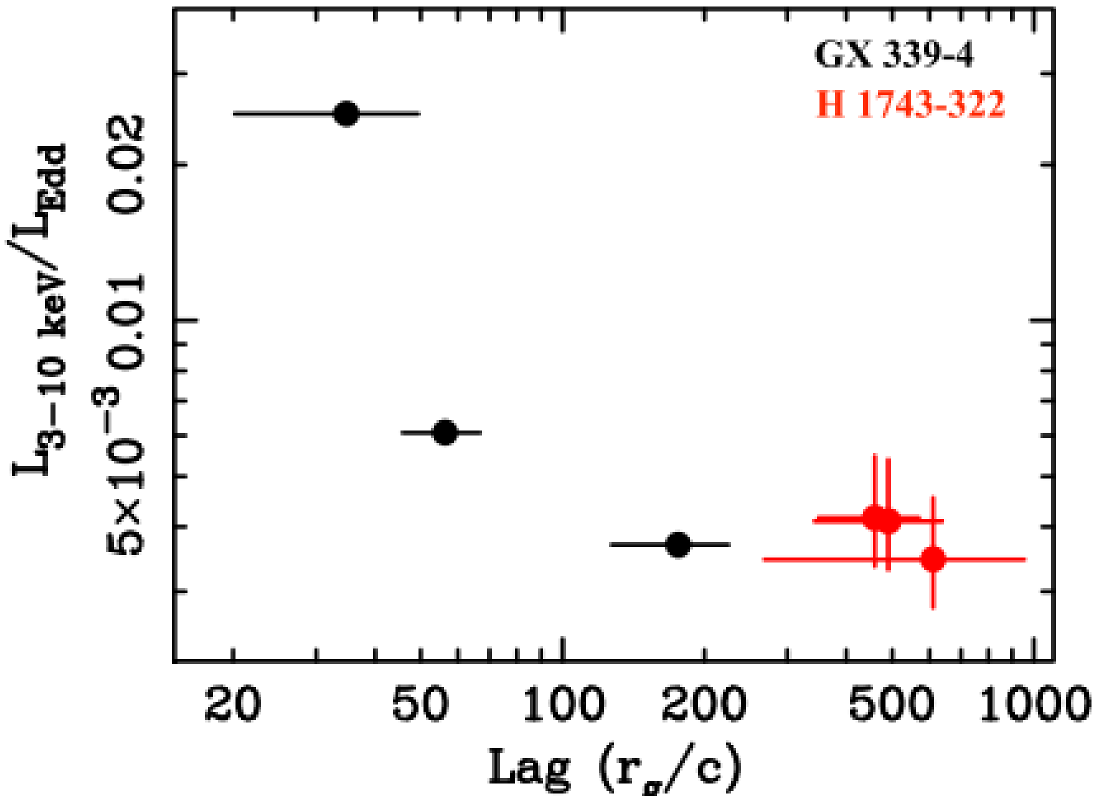

De Marco & Ponti 2016

Plant+ 2014: GX 339–4

Only data >4 keV fitted to avoid complex spectral shape common a low energies.

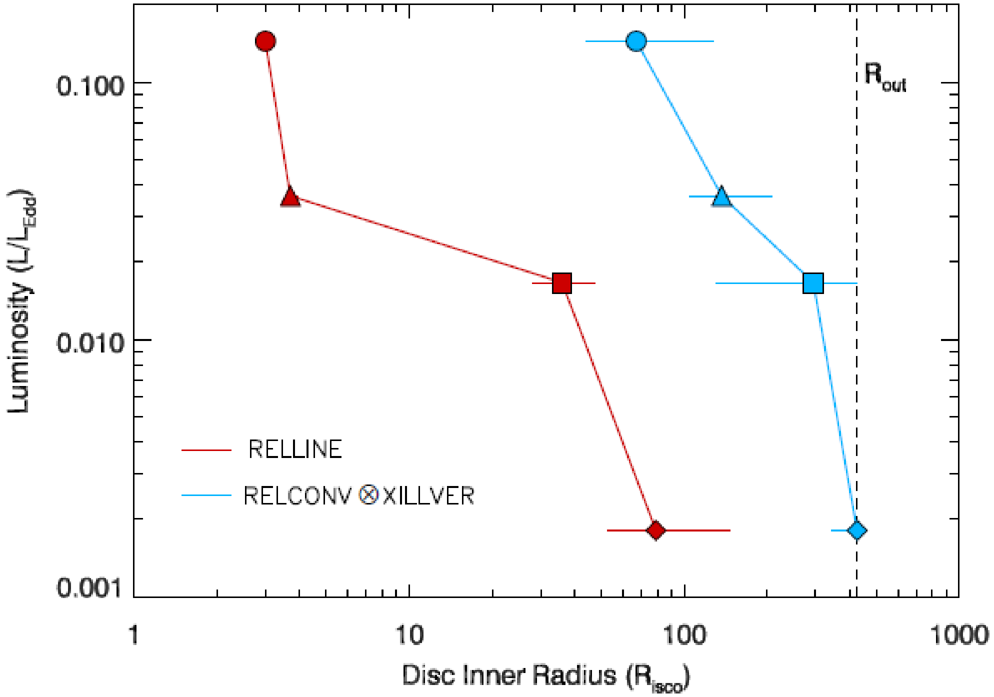

Fig. 3. Evolution of the estimated inner radii (x-axis; Table 3) as a function of luminosity (y-axis; assuming a BH mass and distance of 8 $M_\odot$ and 8 kpc respectively), clearly showing that the inner radius decreases as the source luminosity rises. The red and blue lines refer to fits with RELLINE and RELCONV∗XILLVER respectively. The black dashed line indicates the disc outer radius, which was fixed to be 1000 r_g.

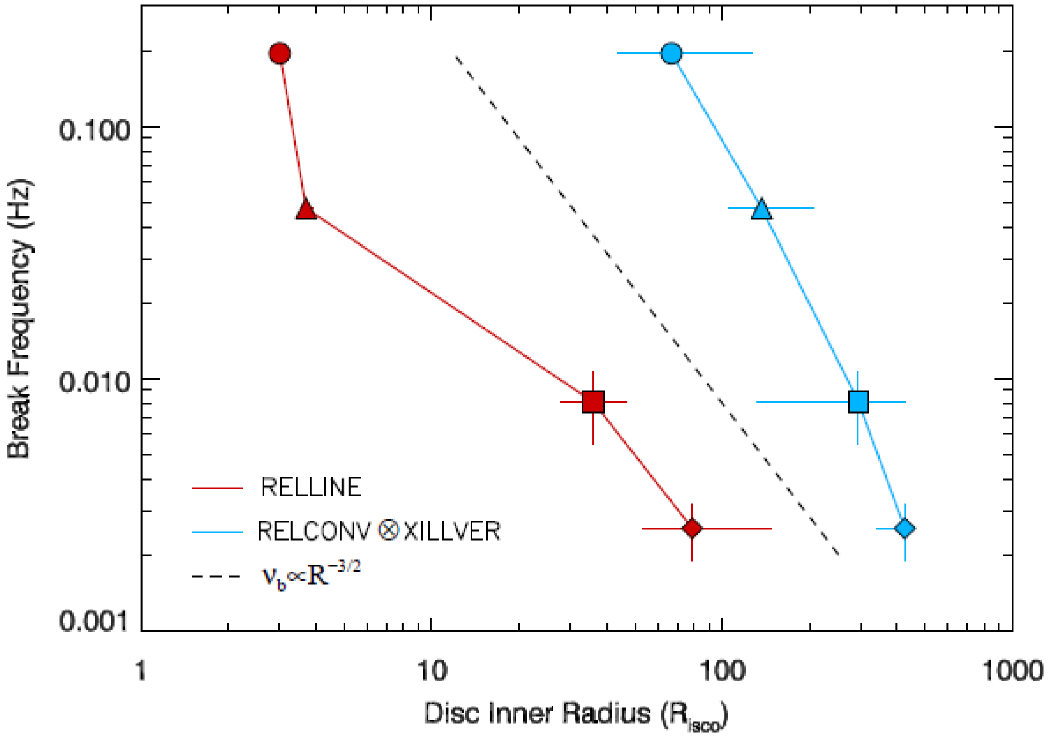

Fig. 9. The estimated disc inner radii (x-axis; Table 3) using RELLINE (red) and RELCONV∗XILLVER (green) versus and the fitted break frequency from simultaneous RXTE observations (y-axis; Table 5). The dotted line represents the relation $\nu \propto R^{-3/2}$, which corresponds to the dynamical and viscous timescales for accretion onto a BH.

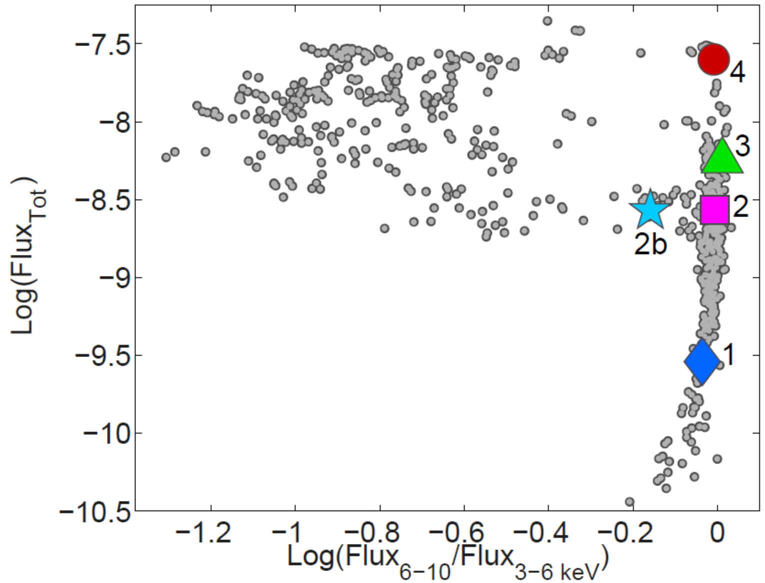

Inner disc radius from *RXTE* data in a bright hard state of GX 339–4, Dziełak, AAZ, et al. 2019

- A set of summed spectra with 10^7 counts (following the method of García+2015), similar to their data set B.
- Garcia+2015 found $R_{\rm in}=1.5^{+0.4}_{-0.2}R_{\rm ISCO}$.
- We find $R_{\rm in} \approx 47_{-45}^{+1000}R_{\rm ISCO}$ in our best model.
- The differences caused by:
  - changes in relxill;
  - their assumption of two different Fe abundances;
  - and addition of an absorption line at 7.2 keV, not seen by any other measurement; we don't see it as well.
- We find only moderate Fe abundance, 2–3 solar.
- Increasing $n_{\rm e}$ to 10^{19} results in an *increase* of $Z_{\rm Fe}$.

The used data selection

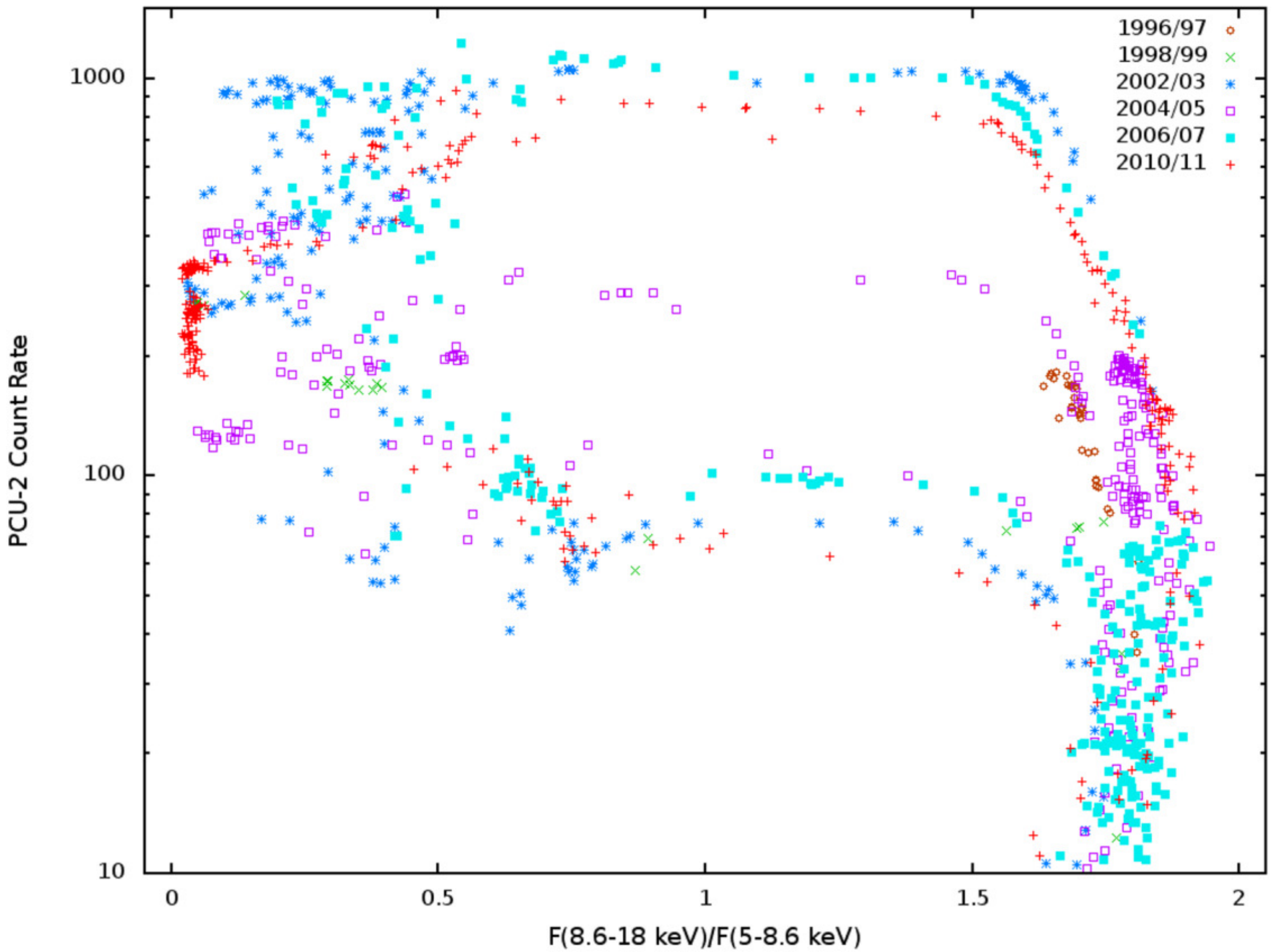

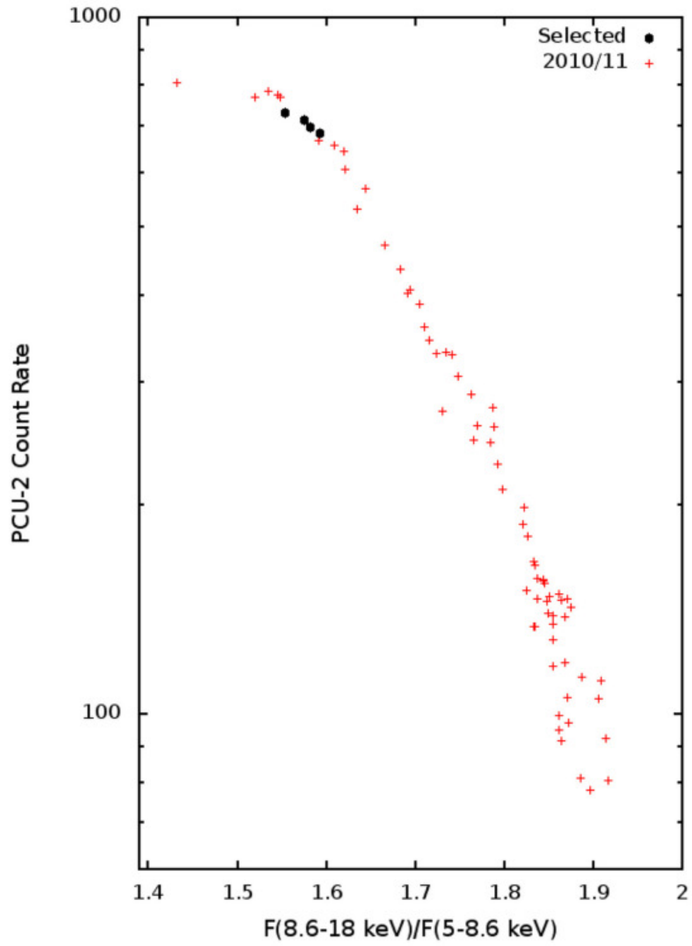

Similar to the data set B of Garcia+2015, but we used observations from a single outburst only.

RXTE data in a bright hard state of GX 339–4

Dziełak, AAZ, et al. 2019

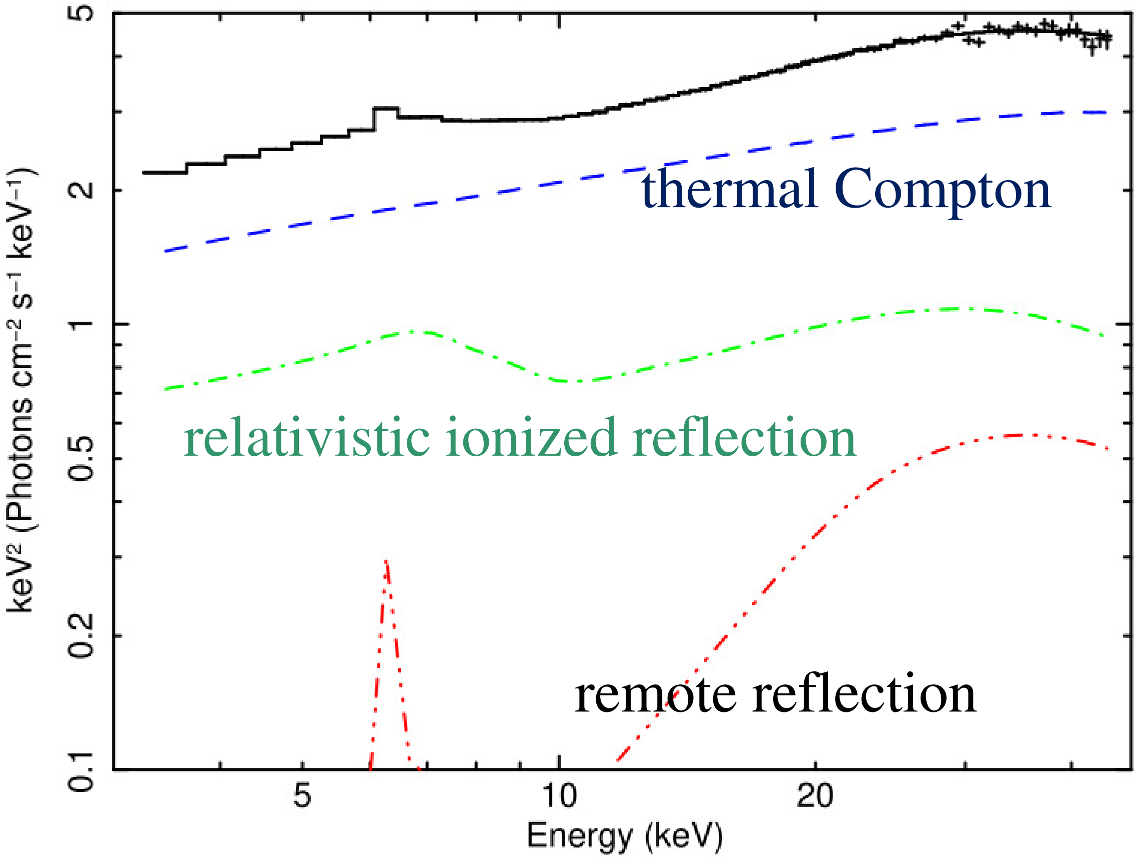

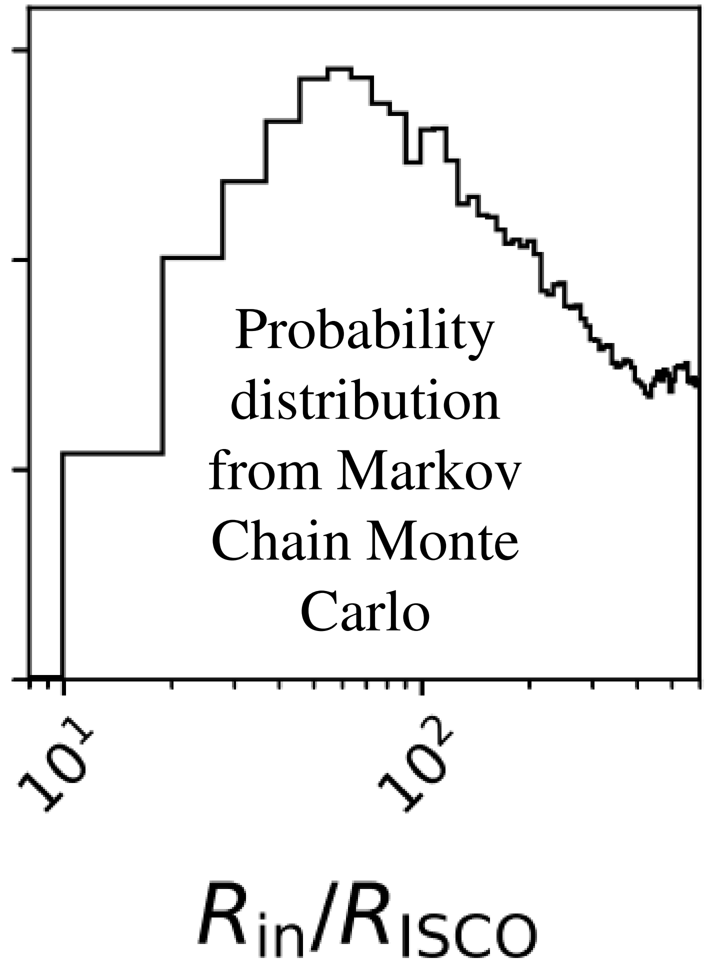

Fit results

Table 1. The spectral fitting results for our models applied to data set G. Model 0 follows the original assumptions of G15, which appear unphysical, and model 6 is our best model, with a physical primary continuum from thermal Comptonization. All models have the ISM absorption term `tbabs`. Model 0: `[relxill(free` $Z_{\rm Fe}$`)+xillver(`$Z_{\rm Fe}$`=1)]gabs`; Models 1 and 2: `relxill+xillver`; Model 3: `relxillD+xillverD`; Models 4 and 5: `reflkerrExp+hreflectExp`; Model 6: `reflkerr+hreflect`. Models 0, 1, 3, 4, and 6 have high and low ionization values for the close and distant reflectors, respectively, while models 2 and 5 have the ionization structure reversed. The effect of scattering of the reflection component is taken into account in separate models with `simplcut` (see Section 3), for which we give here the values of the scattering fraction, $f_{\rm sc}$, in the last row of the table.

Parameter/model	0	1	2	3	4	5	6
$N_{\rm H}/10^{21}$ cm^{-2}	$5.2^{+1.8}_{-1.2}$	$4.7^{+1.5}_{-0.3}$	$6.5^{+1.3}_{-1.7}$	$6.1^{+0.7}_{-0.6}$	$4.4^{+1.9}_{-0.4}$	$6.4^{+0.8}_{-1.1}$	$4.3^{+0.5}_{-0.3}$
Γ	$1.70^{+0.07}_{-0.04}$	$1.66^{+0.03}_{-0.04}$	$1.72^{+0.02}_{-0.03}$	$1.70^{+0.01}_{-0.05}$	$1.66^{+0.06}_{-0.02}$	$1.72^{+0.03}_{-0.01}$	–
y	–	–	–	–	–	–	$1.19^{+0.05}_{-0.08}$
$E_{\rm cut}$/keV	200^{+130}_{-50}	250^{+50}_{-20}	300^{+80}_{-50}	300f	240^{+50}_{-50}	280^{+50}_{-20}	–
$kT_{\rm e}/1$ keV	–	–	–	–	–	–	20^{+3}_{-2}
$R_{\rm in}/R_{\rm ISCO}$	11^{+10}_{-10}	19^{+33}_{-6}	$53^{+\infty}_{-26}$	$55^{+\infty}_{-34}$	15^{+31}_{-12}	$58^{+\infty}_{-28}$	$47^{+\infty}_{-45}$
$Z_{\rm Fe}$	$8.1^{+1.9}_{-5.5}$	$3.1^{+2.0}_{-0.3}$	$2.4^{+0.3}_{-0.2}$	$4.9^{+4.1}_{-0.9}$	$3.9^{+0.8}_{-1.4}$	$2.6^{+0.6}_{-0.4}$	$3.3^{+1.7}_{-1.0}$
i [°]	29^{+31}_{-29}	3^{+33}_{-3}	43^{+17}_{-23}	3^{+43}_{-3}	9^{+32}_{-9}	43^{+21}_{-19}	49^{+34}_{-26}
$\mathcal{R}$ (inner)	$0.059^{+0.001}_{-0.001}$	$0.170^{+0.004}_{-0.005}$	$0.144^{+0.004}_{-0.003}$	$0.059^{+0.033}_{-0.006}$	$0.25^{+0.04}_{-0.19}$	$0.35^{+0.06}_{-0.12}$	$0.42^{+0.36}_{-0.12}$
$\log_{10}\xi$ (inner)	$3.7^{+0.2}_{-0.5}$	$3.9^{+0.1}_{-0.1}$	$0.0^{+2.3}$	$3.7^{+0.1}_{-0.1}$	$3.9^{+0.1}_{-0.1}$	$1.7^{+0.7}_{-1.7}$	$3.9^{+0.1}_{-0.3}$
$\log_{10}\xi$ (outer)	0f	$1.7^{+0.5}_{-1.7}$	$3.8^{+0.2}_{-0.3}$	$0.7^{+1.0}_{-0.3}$	$2.0^{+0.3}_{-0.4}$	$3.7^{+0.1}_{-0.3}$	0f
$n_{\rm e}/1$ cm^{-3}	10^{15}f	10^{15}f	10^{15}f	10^{19}f	10^{15}f	10^{15}f	10^{15}f
$\delta(gabs)$	$0.011^{+0.011}_{-0.009}$	–	–	–	–	–	–
$kT_{\rm bb}/1$ keV	–	–	–	–	–	–	$0.34^{+0.04}_{-0.09}$
χ^2_ν	65.6/61	68.7/61	68.3/61	72.4/62	69.1/61	69.2/61	62.1/61
p_i (AIC)	0.136	0.007	0.008	0.018	0.024	0.023	0.784
$f_{\rm sc}$	$0^{+0.27}$	$0^{+0.29}$	$0^{+0.31}$	$0^{+0.12}$	$0^{+0.26}$	$0^{+0.79}$	$0.30^{+0.15}_{-0.30}$

An open issue: the unabsorbed soft X-ray spectra of BH binaries

- The usual assumption in spectral fitting is to assume there is a disc blackbody component dominating at low energies.
- This may be a good assumption in the soft state, but not in the hard state, where the inner disc is strongly irradiated, for any geometry.
- The unabsorbed soft X-ray spectra in the hard state are poorly determined for most of BH binaries. The usual assumption is that the blackbody-like components are much weaker in νF_ν than the ~100 keV Comptonization peaks, but we don't know for sure because of absorption and instrumental pileup.

The work of our group to resolve this issue

1. GX 339–4 in the hard state with *XMM* (Basak & AAZ 2016). Truncated discs in all cases, different from Miller+2006; Tomsick+2008 (detector pileup), agrees with Plant+2015.
2. GX 339–4 in the hard state with *RXTE* PCA (Dziełak+2019). A truncated disc found for the same data for which García+2015 found the disc close to ISCO (assuming two different Fe abundances in two disc regions).
3. Cyg X-1 with *Suzaku* and *NuSTAR*. The previous study by Parker+2015 used an unphysical spectrum. A truncated disc found (Basak, AAZ, Parker & Islam 2017).
4. New codes for relativistic reflection: reflkerr, hreflect, see users.camk.edu.pl/mitsza/reflkerr; Niedźwiecki+ 2016, 2018, 2019.

Color correction

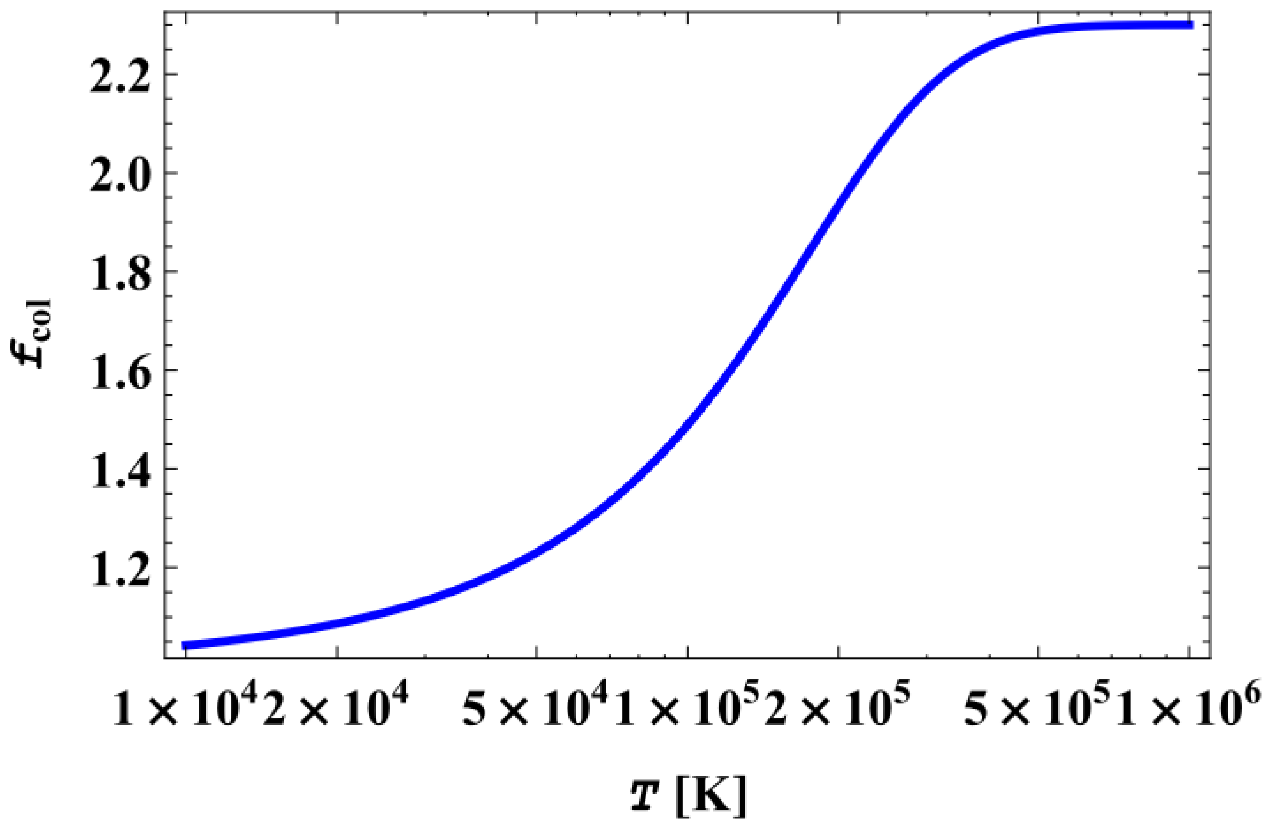

Figure 1. The dependence of $f_{\rm col}$ on the disc temperature from the formula of Chiang (2002) approximating results of Hubeny et al. (2001).

If we measure the reflector density:

- $\xi \equiv 4\pi F_{\rm irr}/n$
- $F_{\rm irr} \sim L/x^2$, where x is the distance between the illuminating source and reflector, of the order of the disc truncation radius.
- $L = 4\pi D^2 F_{\rm obs}$
- Thus, $n = 4\pi F_{\rm irr}/\xi$, which can be compared to the fitted value.

Comparison of the calculated densities vs. those fitted by Jiang+2019a, b, Tomsick+2018

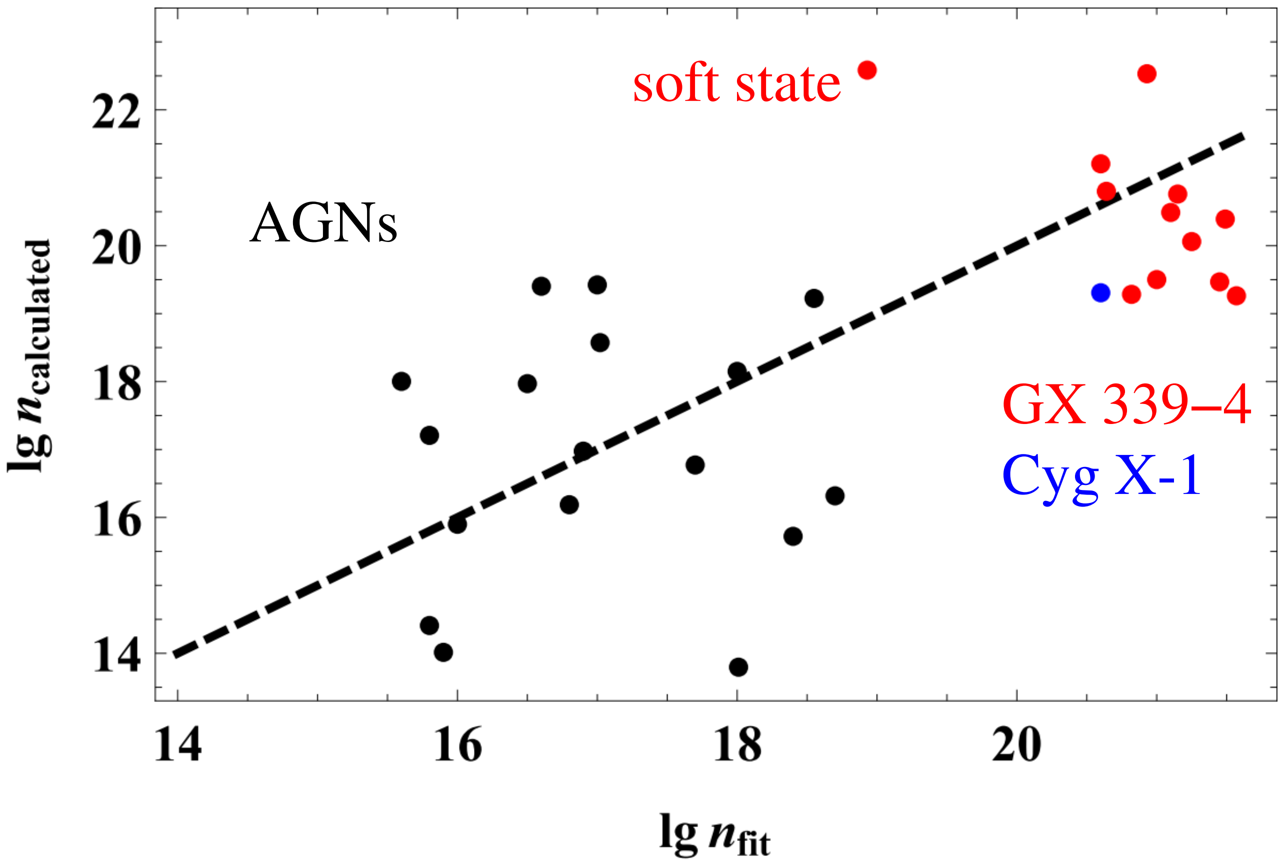

A rough agreement, except for the soft state of GX 339–4.

AAZ+2020

Increasing the density implies an increase of the irradiating flux

$F_{\rm irr} = \xi n/4\pi = (1-{\rm albedo})\sigma T_{\rm eff}^{\ 4}$

$T_{\rm eff} \sim 1$ keV for the brightest hard states of GX 339−4 if the disc extends to ISCO

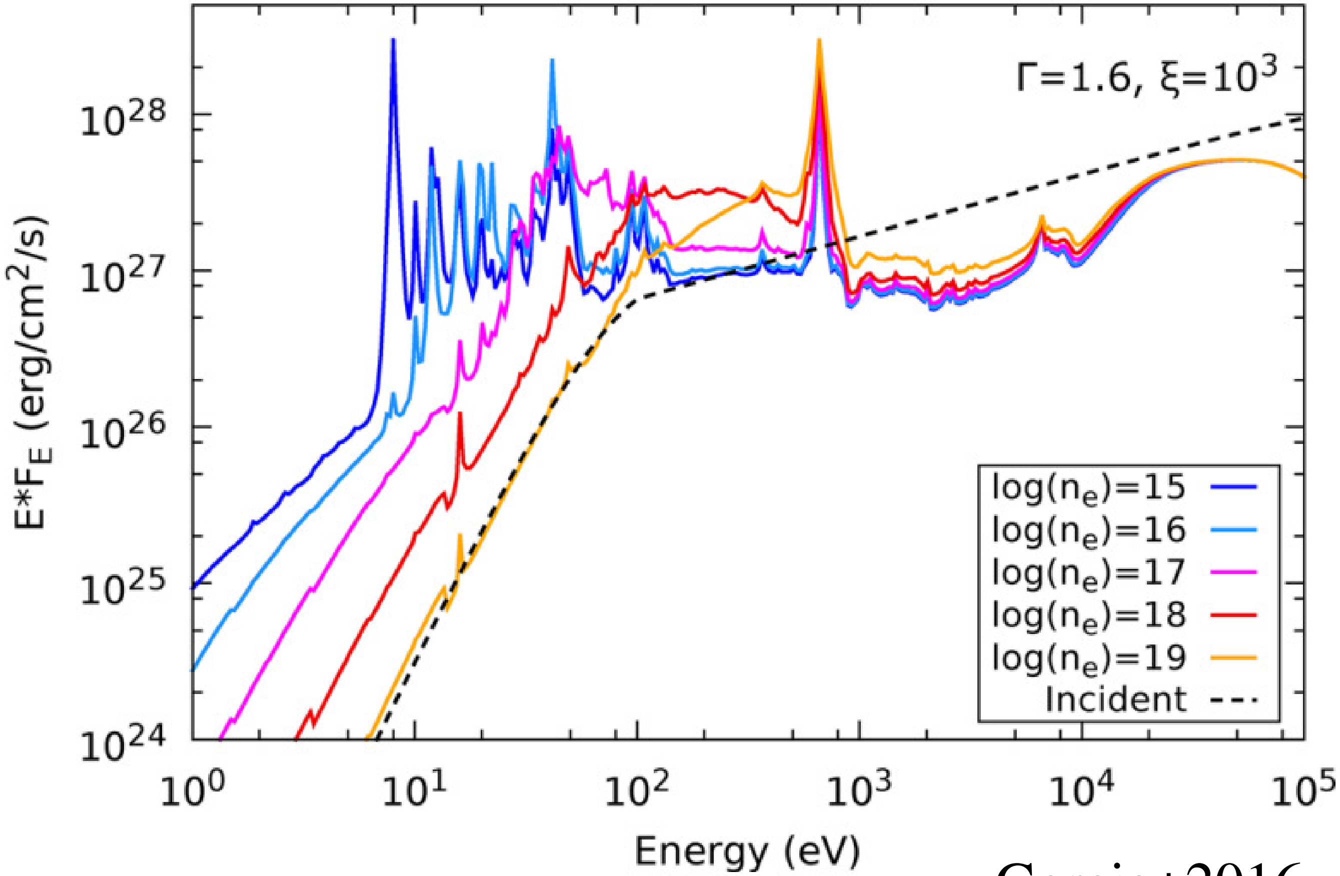

Garcia+2016